Asian Journal of Physics
Vol. 32, Nos 9-12 (2023) 607-613
Available on: www.asianjournalofphysics.com

ap

Analysis and characterization of an octave-bandwidth twin-folded-waveguide slow-wave structure

M Sumathy and Subrata Kumar Datta

Microwave Tube R & D Centre , DRDO, Ministry of Defence ,
Jalahalli, Bangalore - 560 013, India

Dedicated to Prof B N Basu

A novel configuration of folded-waveguide slow-wave structure was conceptualized in which a pair of identical conventional folded-waveguide slow-wave structures is combined in a contra-twined placement (similar to a contra-wound helix or a ring-bar structure). The proposed structure promises cold-bandwidth close to an octave with lowered interaction impedance. The twin-folded configuration would ease out the manufacturing aspects appreciably and also would allow operation with a larger electron beam carrying higher current or requiring lower focusing magnetic field. The reason being a constituent conventional single folded-waveguide structure operating at a low frequency (having larger dimensions), in its twin-folded configuration, would offer operability approximately at double the frequency over almost an octave bandwidth. The analysis of the structure was carried out by parametric approach and validated against numerical simulation and cold-test measurement, for a structure operating at Ka-band and validated against numerical simulation at W-band.

Keywords: Broadbanding, Folded-waveguide slow-wave structure, Twin-folded-waveguide slow-wave structure.
doi.10.54955/AJP.32.9-12.2023.607-613

1 Introduction

Conventionally, a configuration of a folded-waveguide slow-wave structure (FWG-SWS) having a serpentine E-plane bend is known as a serpentine folded-waveguide slow-wave structure (SFWG-SWS). However, cold-bandwidth of these types of structures is typically limited to around 30% [1-4]. Increasing the cold bandwidth of the conventional folded-waveguide slow-wave structure was attempted by ridge and dielectric loading on the broad wall of the structure [5,6]. A new configuration of the conventional folded-waveguide SWS is proposed here as shown in Fig 1 and Fig 2 in which a pair of identical single-folded-waveguide SWSs are combined in a contra-twined placement (similar to a contra-wound helix or a ring-bar structure) [7]. This structure promises cold-bandwidth close to an octave along with moderate interaction impedance suitable for traveling-wave tubes. This new configuration is termed as 'twin-folded-waveguide slow-wave structure (TFWG-SWS)' which supports both symmetric (even) and anti-symmetric (odd) modes: enhancement of axial electric field occurs for the even-mode around the beam-hole region, while axial electric field diminishes around the beam-hole region for the odd-mode. In this paper, detailed analysis and measurements are carried out for obtaining the dispersion and interaction impedance characteristics of the proposed structure. The results from parametric analysis and numerical simulation are compared against experimental results from cold-test measurement.

Corresponding author
e mail: drskdatta@gmail.com (S K Datta)

2 Analysis

Parametric analysis

TFWG-SWS is a periodic structure of periodicity consisting a pair of identical conventional folded-waveguide SWS combined in a contra-twined direction (similar to a contra-wound helix or a ring-bar structure) as shown in Fig 2. The structure comprises two waveguide elements supporting TE10-mode [1-4]: (1) A straight waveguide of length h having broad-wall dimension a, and narrow-wall dimension b accommodating the beam-holes (of radius r_c), and (2) Two E-plane serpentine waveguide bends. The structure can support symmetric modes (even-mode) when each of the folded-waveguides is excited at same phase and anti-symmetric modes (add-modes) when each of the folded-waveguide structures is excited at out-of-phase. Thus, the symmetric mode has the axial electric field for beam-wave interaction; whereas the axial electric field at the beam axis gets cancelled out for the anti-symmetric mode making this mode non-participating for beam-wave interaction. Our interest is, therefore, kept focused on the characteristics of the twin-folded structure operating on symmetric mode.

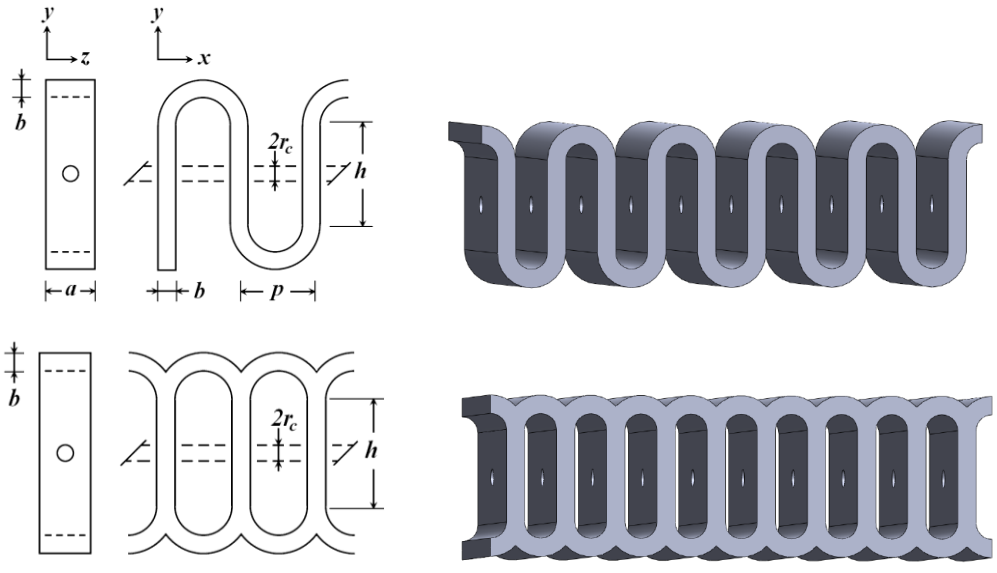

Fig 1. Schematic of typical (a) Single-folded-waveguide and (b) Twin-folded-waveguide slow-wave structures in serpentine.

For a smooth-wall SFWG-SWS, the phase-shift of the axial electric field (along the beam-axis) for the first forward space-harmonic per period can be estimated to be ,

$$\Delta\theta_c = K_c\left(\frac{\omega}{v_{pc}}\right)p + \pi \tag{1}$$

Here, $v_{pc} = \omega/\beta_0$ is the phase velocity of the axial electric field along the beam-axis with β_0 as the axial propagation constant of the axial electric field along the beam-axis. The RF field corresponding to TE_{10} propagating mode in the waveguide undergoes a phase reversal at the bend portion thereby reducing the actual path length of wave propagation. Thus, the axial propagation constant along the beam axis for the TFWG-SWS can be expressed as,

$$\beta_0 = \left(\frac{\theta}{p}\right) = \left(\frac{(\omega^2-\omega_s^2)}{c}\right)^{1/2}\left(\frac{h-b}{p}\right) + \frac{\pi}{p} \tag{2}$$

Here, ω is the angular frequency, ω_s is the cut-off frequency of the structure, and c is the velocity of electromagnetic wave in free space. The capacitance per period of the TFWG-SWS operating on symmetric mode will become half compared to the conventional SFWG-SWS. With this consideration, the cut-off frequency of the TFWG-SWS supporting fundamental TE10-mode is expressed as:

$$\omega_s = \sqrt{2}\,\pi c/a \tag{3}$$

Substituting Eq (3) into Eq (2), one can compute the dispersion characteristics of the structure. The analytical expression for the interaction impedance can be expressed following the approach in [1] and [2] as,

$$K_c = \pi \frac{240}{\sqrt{2}} \frac{\lambda_g}{\lambda_0} \frac{b}{a} \left| \frac{\sin(\beta_o b/2)}{(\beta_o b/2)} \right|^2 \left(\frac{1}{\beta_o p} \right)^2 \tag{4}$$

Here, λ_g is the guided wavelength and λ_0 is the free space wavelength. Using Eqs (2) and (4), one can compute the dispersion and interaction impedance characteristics of the structure.

3D electromagnetic simulation

Electromagnetic simulation of the structure has been carried out using 3D electromagnetic code CST Microwave studio [8] to compute its dispersion and interaction impedance characteristics. The TFWG-SWS was modeled for nine periods and was solved for Eigen frequencies using adaptive mesh refinement. The fundamental symmetric and anti-symmetric modes have been identified by their field configurations. The phase of axial electric field on the beam-axis remains the same at each half of the circuit (lower and upper halves) for the even mode (symmetric) as shown in Fig 2(a), whereas that remains out-of- phase for the odd mode (anti-symmetric) as shown in Fig 2(b).

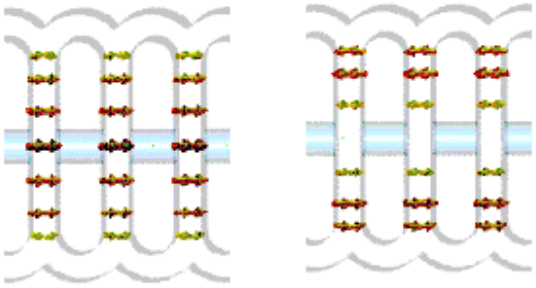

(a) (b)

Fig 2. Two dimensional sectional view of a three period twin-folded-waveguide SWS showing the electric field arrow plot for (a) even mode, (b) odd mode at phase-shift.

The Eigen-frequencies were interpreted for the dispersion characteristics of the structure for the fundamental forward space-harmonic. It is worth mentioning here that both the even- and odd-modes would have the same phase velocity, however, the characteristic impedances would differ. The on axis interaction impedance was computed for the symmetric mode using the relation,

$$K_c = \frac{|E_z^2|}{2\beta_o^2 W v_g} \tag{5}$$

Here, E_z is the axial electric field at the beam-axis obtained from the spatial Fourier decomposition of the total on-axis axial field, W is the energy stored per period and v_g ($= d\omega/d\beta_o$) is the effective axial energy velocity.

3 Cold-test measurement

A Ka-band structure has been fabricated by CNC milling in two halves with a beam hole at center as shown in Fig 3, and the cold-test was carried out after assembling the two halves with suitable probe-coupling. Two co-axial probes are attached parallel to the electric field lines at both the ends of the structure, for measuring its resonance peaks. The cold-test was carried out by conventional resonant perturbation technique. The axial phase shift is determined by measuring the resonant peaks in the frequency domain, based on the return loss/insertion loss resonance peaks, and interpreted for the dispersion characteristics.

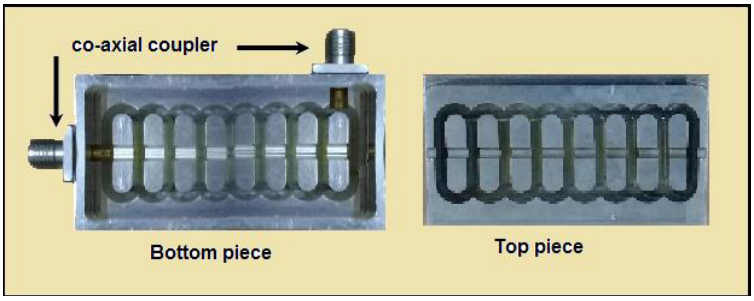

Fig 3. Fabricated Cold-test circuit of the Ka-band twin-folded-waveguide slow-wave structure.

The interaction impedance is measured using the value of perturbation in the resonance peaks by inserting a dielectric rod through the beam-hole at the location of the maximum electric field. The interaction impedance is computed using the following equtation [9],

$$K_c = \left(\frac{2\Delta\beta}{\beta_o}\right) \frac{1}{\varepsilon_0(\varepsilon_r - 1)\pi r_b^2 \beta_o \sin^2(\pi r_b / r_c)} \tag{6}$$

Here, β_o is the effective axial propagation constant of the un-perturbed circuit; $\Delta\beta_o$ is the change in propagation constant due to perturbation; r_b is the radius of the dielectric rod; r_c is the inner radius of the beam-hole; ε_0 and ε_r are the free space permittivity and relative permittivity of the perturbing rod, respectively.

4 Results and discussion

For numerical appreciation of the analysis, a typical TFWG-SWS operating in Ka-band has been considered, in which the constituent single SFWG-SWS operates in the Ku-band. The dispersion and interaction impedance characteristics of these structures as obtained from the 3D electromagnetic analysis are shown in Fig 4. It is evident that the constituent Ku-band SFWG-SWS offers a cold bandwidth of around 36%, while cold bandwidth around an octave could be achieved in its twin-folded configuration, however, at the cost of lower interaction impedance. The TFWG-SWS, however, offers reasonable value of interaction impedance for practical purposes except at the frequencies close to the cut-offs. The interaction impedance can be further improved by the introduction of ferrules near the beam-hole region, which we have kept outside the purview of the present study. Moreover, the circuit having dimensions of Ku-band waveguide would be able to support larger diameter electron beam carrying higher beam current or requiring lower focusing magnetic field.

The dispersion and interaction impedance characteristics for the TFWG-SWS using the parametric analysis are compared with those obtained from the 3D electromagnetic analysis in Fig 5. The measured dispersion and interaction impedance characteristics of the SWS are also superimposed in Fig 5.

Similarly, a TFWG-SWS operating in D-band has been considered, in which each constituent SFWG-SWS operates in the W-band. The comparison of dispersion and interaction impedance characteristics

of these structures as obtained from the parametric analysis and 3D electromagnetic analysis are shown in Fig 6.

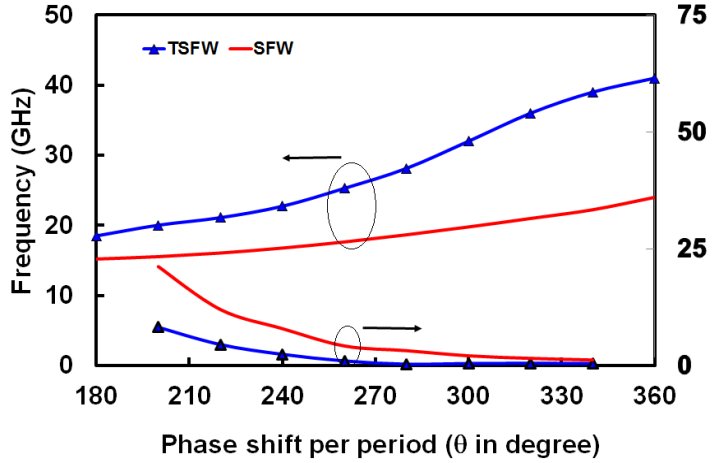

Fig 4. Comparison of dispersion and interaction impedance characteristics of an SFWG structure against those of a TFWG structure.

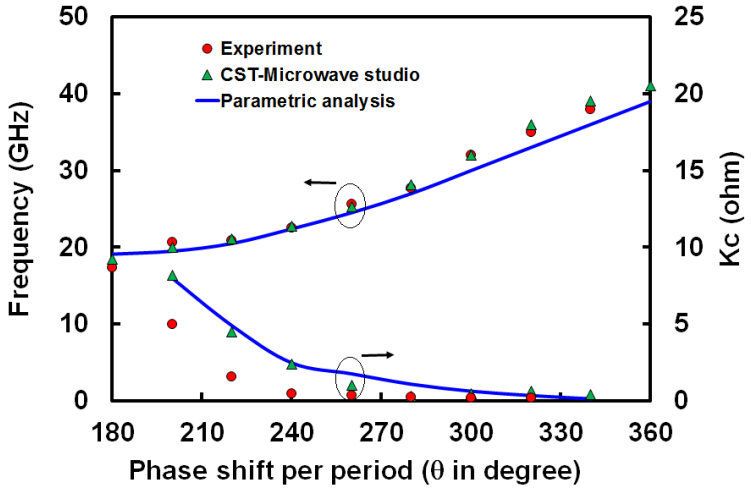

Fig 5. Comparison of dispersion and interaction impedance characteristics of the Ka-band TFWG structure as obtained from parametric analysis, 3D simulation using CST Microwave Studio and measurement of the experimental circuit.

The dispersion characteristics obtained from the parametric analysis and measurement show around 3% and 1% departures, respectively, against those from the 3D electromagnetic analysis; and the interaction impedance characteristics obtained from the parametric analysis and measurement show around 24 % and 22 % departures, respectively, against those from the 3D electromagnetic analysis at center frequency for Ka-band structure. Similarly, the dispersion characteristics obtained from the parametric analysis shows around 3% departures against 3D numerical analysis, and interaction impedance characteristics obtained from the parametric analysis shows 20% departures against 3D numerical analysis, respectively, for the W-band structure. However the percentage error is high at cut-off points. The appreciable deviation in

the measured values of the interaction impedance with regard to analysis is attributed to the higher order waveguide modes and other asymmetric hybrid modes supported in the structure.

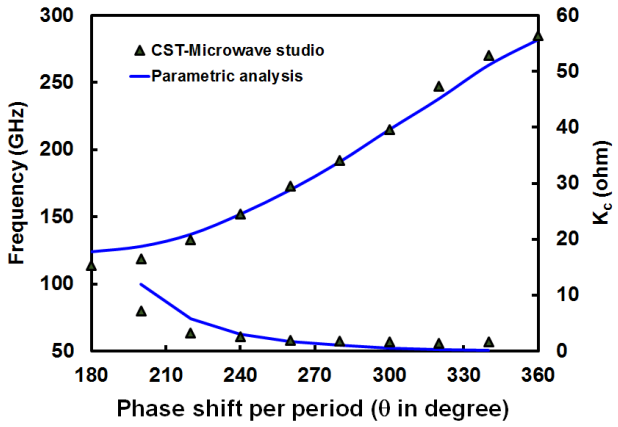

Fig 6. Comparison of dispersion and interaction impedance characteristics of the D-band TFWG structure as obtained from parametric analysis and 3D simulation using CST Microwave Studio.

5 Conclusion

The novel slow-wave structure proposed here can provide close to an octave bandwidth with reasonable interaction impedance. Moreover, the dimensions of the structure would be larger and easy to manufacture; for instance an SFWG-SWS designed at W-band can be used at D-band in its twin-folded configuration. Further, constituent circuit having higher transverse dimensions can be operable with electron beam of larger diameter carrying higher beam current or requiring lower focusing magnetic field. However, the effects of higher order modes and RF loss at higher frequencies are kept outside the purview of the present study. It is expected that the concept would be useful in enhancing the bandwidth and output power of millimeter-wave folded-waveguide devices.

Acknowledgment

Authors are thankful to the Centre Head MTRDC for kind support to carry out the work and necessary permission to publish the work.

References

1. Hutter R G E, Beam and Wave Electronics in Microwave tubes, (New York: Van Nostrand), 1960.
2. Na Y H, Chung S W, Choi J J, Analysis of a broadband Q-band folded-waveguide traveling-wave tube, *IEEE Trans Plasma Sci*, 30(2002)1017–1023.
3. Han S T, Kim J, Park G S, Design of folded waveguide traveling-wave tube, *Microw Opt Technol Lett*, 38(2003) 161–165.
4. Booske J H, Converse M C, Kory C L, Chevalier C T, Gallagher D A, Kreischer K E, Heinen V O, Bhattacharjee S, Accurate parametric modeling of folded waveguide circuits for millimeter-wave traveling wave tubes, *IEEE Trans Electron Devices*, 52(2005)685–694.
5. Sumathy M, Vinoy K J, Datta S K, Analysis of ridge-loaded folded-waveguide slow-wave structure for broad band traveling-wave tubes, *IEEE Trans Electron Devices*, 37(2010)345–349.
6. Zhang C, Gong Y, Gong H, Wei Y, Wang W, Investigation of the dielectric-loaded folded waveguide traveling-wave tube amplifier, *J Infrared Millim Terahertz Waves*, 30(2009)1027–1037.

7. Indian Patent: Twin-Folded-Waveguide Slow-Wave Structure for Traveling-Wave Tube, Patent No. 322394
8. Computer Simulation Technique (CST), GmbH. Online: www.cst.de
9. Sumathy M, Vinoy K J, Datta S K, Non resonanat perturbation formula for measurement of interaction impedance of folded-waveguide slow-wave stucture, Proc IEEE International Vacuum Electronics Conference, 2010, p 98.

[*Received*: 14.05.2023; *accepted*: 05.08.2023]